The suppression of Curie temperature by Sr doping in diluted ferromagnetic semiconductor $(La_{1-x}Sr_x)(Zn_{1-y}Mn_y)AsO$

2014 EPL 107 17004

(http://iopscience.iop.org/0295-5075/107/1/17004)

A Letters Journal Exploring the Frontiers of Physics

July 2014

EPL, **107** (2014) 17004 www.epljournal.org
doi: 10.1209/0295-5075/107/17004

The suppression of Curie temperature by Sr doping in diluted ferromagnetic semiconductor $(La_{1-x}Sr_x)(Zn_{1-y}Mn_y)AsO$

Cui Ding[1], Xin Gong[1], Huiyuan Man[1], Guoxiang Zhi[1], Shengli Guo[1], Yang Zhao[2,3], Hangdong Wang[4], Bin Chen[4] and F. L. Ning[1(a)]

[1] *Department of Physics, Zhejiang University - Hangzhou 310027, China*
[2] *NIST center for Neutron Research, National Institute of Standards and Technology - Gaithersburg, MD 20899, USA*
[3] *Department of Materials Science and Engineering, University of Maryland - College Park, MD 20742, USA*
[4] *Department of Physics, Hangzhou Normal University - Hangzhou 310016, China*

received 11 April 2014; accepted in final form 14 June 2014
published online 7 July 2014

PACS 75.50.Pp – Magnetic semiconductors
PACS 75.47.Lx – Magnetic oxides
PACS 75.30.Cr – Saturation moments and magnetic susceptibilities

Abstract – $(La_{1-x}Sr_x)(Zn_{1-y}Mn_y)AsO$ is a two-dimensional diluted ferromagnetic semiconductor that has the advantage of decoupled charge and spin doping. The substitution of Sr^{2+} for La^{3+} and Mn^{2+} for Zn^{2+} into the parent semiconductor LaZnAsO introduces hole carriers and spins, respectively. This advantage enables us to investigate the influence of carrier doping on the ferromagnetic ordered state through the control of Sr concentrations in $(La_{1-x}Sr_x)(Zn_{0.9}Mn_{0.1})AsO$. 10% Sr doping results in a ferromagnetic ordering below $T_C \sim 30$ K. Increasing Sr concentration up to 30% heavily suppresses the Curie temperature and saturation moments. Neutron scattering measurements indicate that no structural transition occurs for $(La_{0.9}Sr_{0.1})(Zn_{0.9}Mn_{0.1})AsO$ below 300 K.

Introduction. – The observation of ferromagnetic ordering in III-V (Ga,Mn)As below a Curie temperature $T_C \sim 60$ K by Ohno *et al.* [1] has generated extensive research into the diluted ferromagnetic semiconductors (DFS). After almost two decades of efforts, T_C has been improved to as high as 200 K with a Mn doping level of $\sim 12\%$ [2–5]. This temperature is still far below the room temperature which is the prerequisite for the practical application of spintronics [6]. Improving T_C in homogenous (Ga,Mn)As thin films is one of the objectives in the research of DFS. On the other hand, understanding the mechanism of ferromagnetic ordering is hindered by some inherent difficulties. In (Ga,Mn)As, the substitution of Mn^{2+} for Ga^{3+} provides not only local moments but also hole carriers. It is generally believed that ferromagnetic ordering can arise only when spins are effectively mediated by carriers [7]. However, during the fabrication of (Ga,Mn)As thin films, some Mn atoms enter interstitial sites and behave as a double doner, which make it difficult to determine precisely the amount of Mn that substitute Ga at ionic sites. Seeking for new ferromagnetic semiconductor systems with more controllable charge and spin densities might be helpful to understand the general mechanism of ferromagnetism in DFS.

Recently, several bulk DFS systems that are derivatives of Fe-based high-temperature superconductors have been reported. The first Fe-based superconductor is the 1111-type oxypnictide, $LaFeAs(O_{1-x}F_x)$ [8], which has a superconducting transition temperature $T_c = 26$ K. With identical two-dimensional crystal structure, three 1111-type DFS systems, (La,Ba)(Zn,Mn)AsO with $T_C \sim 40$ K [9], (La,Ca)(Zn,Mn)SbO with $T_C \sim 40$ K [10], (La,Sr)(Cu,Mn)SO [11] with $T_C \sim 210$ K have been reported. Similarly, two bulk form DFS systems, $(Ba,K)(Zn,Mn)_2As_2$ [12] with $T_C \sim 180$ K and $(Ba,K)(Cd,Mn)_2As_2$ with $T_C \sim 17$ K [13], have been reported. These two systems are structurally identical to the 122-type iron pnictides superconductor, $(Ba,K)Fe_2As_2$ ($T_c = 38$ K) [14]. The third DFS family reported recently is Li(Zn,Mn)Pn (Pn = P, As) [15,16] with $T_C \sim 50$ K, which is fabricated by doping Mn into the I-II-V direct gap semiconductors LiZnPn (Pn = P, As). LiZnAs can also be viewed as a derivative of the third family of

(a)E-mail: ningfl@zju.edu.cn

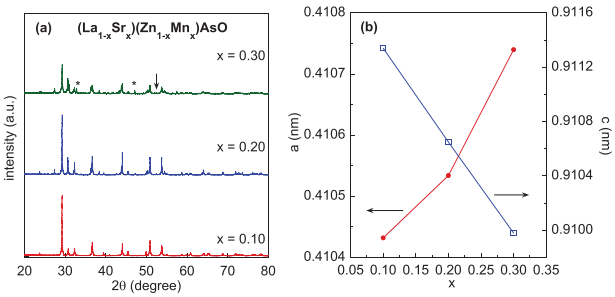

Fig. 1: (Color online) (a) Powder X-ray diffraction pattern of $(La_{1-x}Sr_x)(Zn_{1-y}Mn_y4)AsO$ ($x = y = 0.10, 0.20, 0.30$). Traces of La_2O_3 (↓) and $ZnAs_2$ (∗) impurities are marked for $x = 0.30$. (b) Lattice parameters for the a-axis (red solid circles) and the c-axis (blue open squares).

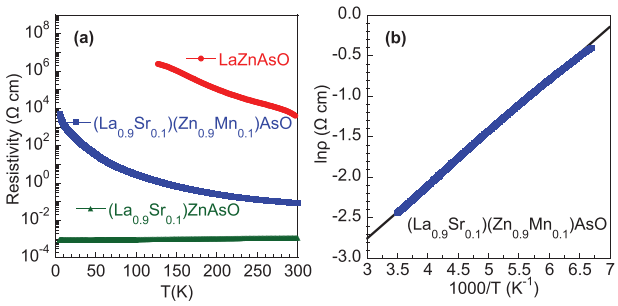

Fig. 2: (Color online) (a) The electrical resistivity for the parent compound LaZnAsO, 10% Sr-doped specimen $(La_{0.9}Sr_{0.1})ZnAsO$, and 10% Sr- and Mn-doped specimen $(La_{0.9}Sr_{0.1})(Zn_{0.9}Mn_{0.1})AsO$. (b) The fitting of resistivity for $(La_{0.9}Sr_{0.1})(Zn_{0.9}Mn_{0.1})AsO$ with an activation function.

Fe-based superconductors LiFeAs ($T_c = 18\,\mathrm{K}$) [17]. The fourth family of Fe-based superconductors is the 11-type $FeSe_{1+\delta}$ ($T_c = 8\,\mathrm{K}$) [18], which can be paralleled to the well-investigated II-VI DFS, *i.e.*, (Zn,Mn)Se. There are two more families of Fe-based superconductors, namely, the 32522-type $(Ca_3Al_2O_5)Fe_2As_2$ ($T_c \sim 30.2\,\mathrm{K}$) [19] and the 42622-type $Sr_4V_2O_6Fe_2As_2$($T_c \sim 37.2\,\mathrm{K}$) [20]. Very recently, the 32522-type DFS $Sr_3La_2O_5(Zn,Mn)_2As_2$ with Curie temperature $T_C \sim 40\,\mathrm{K}$ [21] and the 42622-type DFS $Sr_4Ti_2O_6(Zn,Mn)_2As_2$ with $T_C \sim 25\,\mathrm{K}$ have been reported [22].

Different to thin-film form (Ga,Mn)As specimens, the above new DFS systems are all in bulk form. The availability of a specimen in bulk form enables the investigation of DFS by powerful magnetic probes including NMR (Nuclear Magnetic Resonance), μSR (muon Spin Rotation) and neutron scattering. NMR investigation of I-II-V DFS Li(Zn,Mn)P by Ding *et al.* has shown that the spin-lattice relaxation rate $\frac{1}{T_1}$ of the Li(0) site (zero means that there are no Mn atoms at the N.N. (nearest neighbor) Zn site of Li) exhibits a kink around T_C, which indicates that Li(0) sites are indeed under the influence of ferromagnetic Mn spin fluctuations [23]. Furthermore, $\frac{1}{T_1}$ of the Li(Mn) site is temperature independent above T_C, *i.e.*, $\frac{1}{T_1} \sim 400\,\mathrm{s}^{-1}$, indicating that the Mn spin-spin interaction extends over many unit cells with an interaction energy scale $|J| \sim 100\,\mathrm{K}$. On the other hand, μSR measurements have shown that the bulk form I-II-V, 1111 and 122 DFSs all share a common ferromagnetic mechanism as that of (Ga,Mn)As thin films [9,12,15].

Another important feature of the newly fabricated bulk DFSs is that they all have advantages of decoupled carriers and spins doping. Here the Mn^{2+} substitution for Zn^{2+} introduces only spins, and carriers are introduced at a different site. Only when both carriers and spins are introduced simultaneously, can ferromagnetic ordering develop [9]. In this paper, we dope Sr and Mn into the direct gap parent semiconductor LaZnAsO up to the doping level of 30%. We found that chemical solubility is 20%, which is much higher than 10% of doping Ba. This allows us to investigate the high doping regime in a more reliable manner. The Curie temperature T_C in $(La_{1-x}Sr_x)(Zn_{1-x}Mn_x)AsO$ increases from 30 K of $x = 0.10$ to 35 K of $x = 0.20$, but decreases to 27 K for $x = 0.30$. For a fixed Mn concentration of $x = 0.10$, we found that a higher hole doping than 10% suppresses both T_C and the saturation moments. 30% hole doping suppresses the saturation moment by almost an order, and no strong enhancement in the magnetization curve that corresponds to the ferromagnetic ordering has been observed.

Experiments. – Polycrystalline specimens of $(La_{1-x}Sr_x)(Zn_{1-y}Mn_y)AsO$ were prepared through the solid-state reaction method by mixing intermediate products LaAs, ZnAs, MnAs, ZnO, MnO and SrO with nominal concentrations. The mixture was then made into pellets and heated to 1150 °C slowly. It was kept at 1150 °C for 40 hours before cooling down by shutting off the furnace. The intermediate products LaAs, ZnAs and MnAs were prior produced with mixing high-purity elements La, Zn, Mn and As and heating at 900 °C for 10 hours. The processes of mixing were carried in high-purity Ar atmosphere in a glove box and the mixtures were sealed in an evacuated silica tube before heating. The polycrystals were characterized by X-ray powder diffraction and dc magnetization by SQUID (Superconducting Quantum Interference Device). The electrical resistance was measured on sintered pellets with the typical four-probe method. Neutron scattering measurements were performed at NIST Center for Neutron Research (NCNR) using the BT-1 powder Diffractometer.

Results and discussion. – In fig. 1(a), we show the powder X-ray diffraction patterns of $(La_{1-x}Sr_x)(Zn_{1-y}Mn_y)AsO$ with Sr and Mn of equal doping levels ($x = y = 0.10, 0.20, 0.30$). As demonstrated by the Reitveld refinement for the LaZnAsO compound [9], the Bragg peaks of the specimens can be well indexed into a tetragonal crystal structure of space group $P4/nmm$. The lattice parameters for three concentrations are shown in fig. 1(b). The lattice constant

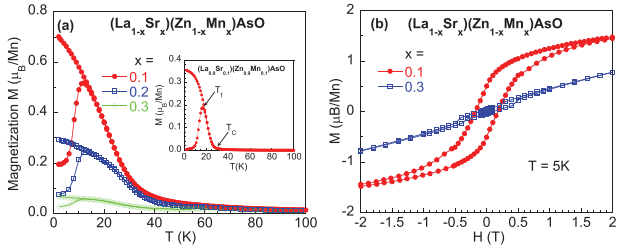

Fig. 3: (Color online) (a) dc magnetization M measured under ZFC and FC conditions for $(La_{1-x}Sr_x)(Zn_{1-y}Mn_y)AsO$ ($x = y = 0.10$, 0.20, 0.30) at $\mu_0 H = 0.1$ T; the inset shows M of $(La_{0.9}Sr_{0.1})(Zn_{0.9}Mn_{0.1})AsO$ measured at $\mu_0 H = 0.005$ T, T_C and T_f are marked by arrows. (b) The isothermal magnetization measurements for $(La_{1-x}Sr_x)(Zn_{1-y}Mn_y)AsO$ ($x = y = 0.10$, 0.30) at 5 K.

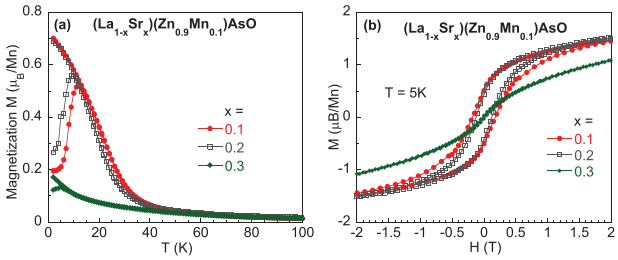

Fig. 4: (Color online) (a) dc magnetization M measured under ZFC and FC conditions for $(La_{1-x}Sr_x)(Zn_{0.9}Mn_{0.1})AsO$ ($x = 0.10$, 0.20, 0.30) at $\mu_0 H = 0.1$ T. (b) The isothermal magnetization measurements for $(La_{1-x}Sr_x)(Zn_{0.9}Mn_{0.1})AsO$ ($x = 0.10$, 0.20, 0.30) at 5 K.

a monotonically increases while c monotonically decreases with Sr and Mn doping, indicating a successful solid solution of (La,Sr) and (Zn,Mn). We find the chemical solubility is as high as 20%, much higher than the case of Ba and Mn doping into LaZnAsO which is only 10% [9]. This can be attributed to the much closer atomic radius of La^{3+} (0.106 nm) and Sr^{2+} (0.113 nm). Traces of La_2O_3 ($\downarrow$) and $ZnAs_2$ ($*$) impurities are observed for $x = 0.30$ concentration. These impurities are non-magnetic and do not affect our discussion below.

We show the results of the electrical resistance measured for the parent compound LaZnAsO, 10% Sr-doped specimen $(La_{0.9}Sr_{0.1})ZnAsO$, and 10% Sr- and Mn-doped specimen $(La_{0.9}Sr_{0.1})(Zn_{0.9}Mn_{0.1})AsO$ in fig. 2. The parent compound is a direct gap semiconductor with a band gap of $\sim$ 1.5 eV [24], and it displays a typical semiconducting behavior. 10% Sr substitution for La readily changes the semiconductor into a metal, as demonstrated by decreasing resistivity with decreasing temperature. More interestingly, once 10% Mn are doped into $(La_{0.9}Sr_{0.1})ZnAsO$, the specimen returns to a semiconducting behavior. It seems that spins induced by Mn atoms localize the hole carriers. We do a tentative fitting of the $\rho(T)$ data for $(La_{0.9}Sr_{0.1})(Zn_{0.9}Mn_{0.1})AsO$ near room temperature with a thermally activated conductivity, $\frac{1}{\rho} = C\exp(-E_a/2k_BT)$. The fitting is good, and the scenario of the disorder-induced localization mechanism seems not applicable here. We also find an activation energy of 0.056 eV, which is much smaller than the gap energy of LaZnAsO.

In fig. 3(a), we show the dc magnetization curve of $(La_{1-x}Sr_x)(Zn_{1-y}Mn_y)AsO$ ($x = y = 0.10$, 0.20, 0.30) measured with 0.1 T external field under zero-field-cooled (ZFC) and field-cooled (FC) conditions (note that Sr atoms and Mn are in the same doping level). We define the Curie temperature of ferromagnetic ordering, T_C, as the temperature where the magnetization curve measured at 0.005 T displays a sharp enhancement, as marked by the arrow in the inset of fig. 3(a). As the doping level increases, T_C increases from 30 K for $x = 0.10$ to 35 K for $x = 0.20$, and then decreases to 27 K for $x = 0.30$. The saturation moment is 0.71 μ_B/Mn for $x = 0.10$, which is comparable to that of $(La_{0.9}Ba_{0.1})(Zn_{0.9}Mn_{0.1})AsO$ [9]. The saturation moment is suppressed monotonically to 0.07 μ_B/Mn at the doping level of $x = 0.30$. Another feature of the magnetization curve is that ZFC and FC curves split at a temperature below T_C, as marked by the arrow in the inset of fig. 3(a). This temperature is defined as T_f, which is the onset temperature of static spin freezing, as has been investigated by the μSR measurement of (La,Ba)(Zn,Mn)AsO [9]. T_f decreases monotonically from 17 K ($x = 0.10$) to 12 K ($x = 0.30$).

The isothermal magnetization at 5 K for $(La_{0.9}Sr_{0.1})(Zn_{0.9}Mn_{0.1})AsO$ and $(La_{0.7}Sr_{0.3})(Zn_{0.7}Mn_{0.3})AsO$ is shown in fig. 3(b). With the increase of Sr and Mn concentrations, the coercive fields are quickly suppressed from 0.178 T to 0.102 T. For comparison, the coercive field of $(Ga_{0.965}Mn_{0.035})As$ is $\sim$ 0.005 T [1]. On the other hand, the saturation remanence of $(La_{0.9}Sr_{0.1})(Zn_{0.9}Mn_{0.1})AsO$ is $\sim$ 0.5 μ_B/Mn, an order of magnitude larger than $\sim$ 0.04 μ_B/Mn of $(La_{0.7}Sr_{0.3})(Zn_{0.7}Mn_{0.3})AsO$. The suppression of T_C, saturation moments, and coercive fields with higher Mn doping levels is very likely arising from the competition of the direct antiferromagnetic exchange interaction from N.N. Mn atoms at Zn sites. The probability to find two Mn at N.N. Zn sites is $P(N;x) = C_N^4 x^N (1-x)^{(4-N)} = 29.16\%$ for $x = 0.10$ (where $N = 1$ and $x = 0.10$). This probability increases to 41.16% for the doping level of $x = 0.30$. The direct antiferromagnetic coupling between Mn-Mn pairs eventually results in the antiferromagnetic ordering in LaMnAsO at $T_N = 317$ K [25].

Since we can control spins and carriers separately, it will be interesting to investigate the influence of different carrier doping levels on the magnetic state at a fixed Mn concentration. We fix Mn at the level of 0.10, and enhance the doping levels of Sr up to 20% and 30%. The ZFC and FC dc magnetization curves of three specimens are plotted in fig. 4(a) and their isothermal magnetizations at 5 K are plotted in fig. 4(b). Compared to the 10% Sr doping sample, both T_C and saturation moments are only slightly suppressed with 20% Sr doping. When

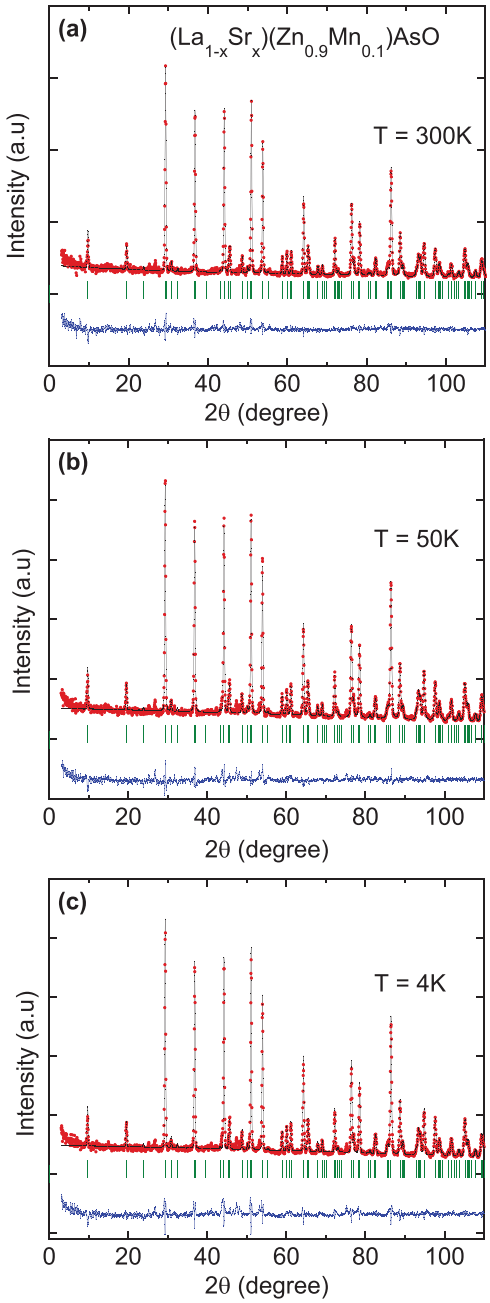

Fig. 5: (Color online) Neutron diffraction pattern for the powder specimen of $(La_{0.9}Sr_{0.1})(Zn_{0.9}Mn_{0.1})AsO$ at 300 K (a), 50 K (b) and 4 K (c) at NIST. Error bars are smaller than plot symbols.

the Sr doping level is increased to $x = 0.30$, both T_C and saturation moments are heavily suppressed. The saturation moment decreases from 0.71 μ_B/Mn for $x = 0.10$ to 0.17 μ_B/Mn for $x = 0.30$. Similarly, T_f decreases from 17 K to 5 K and the coercive field declines from 0.178 T to 0.022 T. The saturation remanence decreases from ~ 0.5 μ_B/Mn for $x = 0.10$ to 0.03 μ_B/Mn for $x = 0.30$. In the early stage of DFS research, it has been theoretically proposed that spins are mediated by hole carriers through the RKKY interaction [7]. We can write the RKKY exchange interaction as $J \sim \frac{\cos(2k_F r)}{r^3}$, where k_F is the radius of the Fermi surface if assuming the Fermi surface is a spherical shape, and r the distance between two localized moments. The first oscillation period of the RKKY interaction supports ferromagnetic coupling. In the present work, doping more Sr into $(La_{1-x}Sr_x)(Zn_{0.9}Mn_{0.1})AsO$ has introduced extra hole carriers, which modifies the density of states and the Fermi surface, and subsequently the ferromagnetic ordering.

To investigate the spin structure, we conducted neutron diffraction of the powder specimen $(La_{0.9}Sr_{0.1})(Zn_{0.9}Mn_{0.1})AsO$ (which has the largest saturation moment size) at 4 K, 50 K and 300 K at NCNR, and show the results in fig. 5. We found that the neutron powder diffraction pattern is in line with the X-rays diffraction pattern, and no impurities are observed. This indicates that Mn atoms are indeed substituted into Zn sites. We spent 8 hours for a 3 grams sample at 4 K, but still could not separate the magnetic diffraction peaks from the structural ones. In $(La_{0.9}Sr_{0.1})(Zn_{0.9}Mn_{0.1})AsO$, the average moment size is only $\sim 0.07\,\mu_B$/Mn(Zn), which is smaller than the limit of neutron resolution $\sim 0.1\,\mu_B$ with the current experiment configuration. Nonetheless, we do not observe a structural phase transition from 300 K to 4 K, which crosses $T_C = 30$ K.

Summary and conclusion. – To summarize, we successfully synthesized a new DFS system $(La_{1-x}Sr_x)(Zn_{1-x}Mn_x)AsO$ with a doping level up to 30%. The maximum T_C is as high as 35 K at the doping of $x = 0.20$. With the advantage of decoupled spin and carrier doping, we could investigate the influence of the carrier concentration on the ferromagnetic ordering. We found that 30% Sr substitution for La in $(La_{1-x}Sr_x)(Zn_{0.9}Mn_{0.1})AsO$ suppresses the ferromagnetic ordering, leaving a spin-glass-like magnetic ordered state. As we have shown in (LaBa)(ZnMn)AsO [9], spins cannot order ferromagnetically without carrier doping. Our experimental evidence shown in this work unequivocally demonstrates that too much carriers suppresses both the Curie temperature and the saturation moments. In other words, too much carriers are detrimental to the ferromagnetic ordering as well. It requires a delicate balance between carriers and spins to achieve the highest T_C. In addition, our neutron scattering experiments rule out the possibility of a structural transition between 300 K and 4 K for $(La_{0.9}Sr_{0.1})(Zn_{0.9}Mn_{0.1})AsO$ specimen. Finally, as stated previously, the common two-dimensional crystal structure shared by ferromagnetic $(La_{1-x}Sr_x)(Zn_{1-y}Mn_y)AsO$, 1111-type Fe-based high-temperature superconductors and antiferromagnetic LaMnAsO, makes it possible to make various junctions through As layers.

* * *

The work at Zhejiang was supported by the National Basic Research Program of China (No. 2014CB921203,

2011CBA00103), NSF of China (No. 11274268). FLN acknowledges helpful discussions with I. Mazin, I. Zutic, Y. J. Uemura and C. Q. Jin.

REFERENCES

[1] Ohno H., Shen A., Matsukura F., Oiwa A., Endo A., Katsumoto S. and Iye Y., *Appl. Phys. Lett.*, **69** (1996) 363.

[2] Wang M., Campion R. P., Rushforth A. W., Edmonds K. W., Foxon C. T. and Gallagher B. L., *Appl. Phys. Lett.*, **93** (2008) 132103.

[3] Chen L., Yan S., Xu P. F., Wang W. Z., Deng J. J., Qian X., Ji Y. and Zhao J. H., *Appl. Phys. Lett.*, **95** (2009) 182505.

[4] Chen L., Yang X., Yang F. H., Misuraca J., Xiong P., Molnar S. V. and Zhao J. H., *Nano Lett.*, **11** (2011) 2584.

[5] Dietl T. and Ohon H., *Rev. Mod. Phys.*, **86** (2014) 187.

[6] Zutic I., Fabian J. and Das Sarma S., *Rev. Mod. Phys.*, **76** (2004) 323.

[7] Dietl T., Ohno H., Matsukura F., Cibert J. and Ferrand D., *Science*, **287** (2000) 1019.

[8] Kamihara Y., Watanabe T., Hirano M. and Hosono H., *J. Am. Chem. Soc.*, **130** (2008) 3296.

[9] Ding C., Man H. Y., Qin C., Lu J. C., Sun Y. L., Wang Q., Yu B. Q., Feng C. M., Goko T., Arguello C. J., Liu L., Frandsen B. A., Uemura Y. J., Wang H. D., Luetkens H., Morenzoni E., Han W., Jin C. Q., Munsie T., Williams T. J., D'Ortenzio R. M., Medina T., Luke G. M., Imai T. and Ning F. L., *Phys. Rev. B*, **88** (2013) 041102(R).

[10] Han W., Zhao K., Wang X. C., Liu Q. Q., Ning F. L., Deng Z., Liu Y., Ding C. and Jin C. Q., *Sci. China Phys. Mech. Astron.*, **56** (2013) 2026.

[11] Yang X. J., Li Y. K., Shen C. Y., Si B. Q., Sun Y. L., Tao Q., Cao C., Xu Z. A. and Zhang F. C., *Appl. Phys. Lett.*, **103** (2013) 022410.

[12] Zhao K., Deng Z., Wang X. C., Han W., Zhu J. L., Li X., Liu Q. Q., Yu R. C., Goko T., Frandsen B., Liu L., Ning F. L., Uemura Y. J., Dabkowska H., Luke G. M., Luetkens H., Morenzoni E., Dunsiger S. R., Senyshyn A., Boni P. and Jin C. Q., *Nat. Commun.*, **4** (2013) 1442.

[13] Yang X. J., Li Y. K., Zhang P., Luo Y. K., Chen Q., Feng C. M., Cao C., Dai J. H., Tao Q., Cao G. H. and Xu Z. A., *J. Appl. Phys.*, **114** (2013) 223905.

[14] Rotter M., Tegel M. and Johrendt D., *Phys. Rev. Lett.*, **101** (2008) 107006.

[15] Deng Z., Jin C. Q., Liu Q. Q., Wang X. C., Zhu J. L., Feng S. M., Chen L. C., Yu R. C., Arguello C., Goko T., Ning F. L., Zhang J. S., Wang Y. Y., Aczel A. A., Munsie T., Williams T. J., Luke G. M., Kakeshita T., Uchida S., Higemoto W., Ito T. U., Gu B., Maekawa S., Morris G. D. and Uemura Y. J., *Nat. Commun.*, **2** (2011) 422.

[16] Deng Z., Zhao K., Gu B., Han W., Zhu J. L., Wang X. C., Li X., Liu Q. Q., Yu R. C., Goko T., Frandsen B., Liu L., Zhang J. S., Wang Y. Y., Ning F. L., Maekawa S., Uemura Y. J. and Jin C. Q., *Phys. Rev. B*, **88** (2013) 081203(R).

[17] Wang X. C., Liu Q. Q., Lv Y. X., Gao W. B., Yang L. X., Yu R. C., Li F. Y. and Jin C. Q., *Solid State Commun.*, **148** (2008) 538.

[18] Hsu F. C., Luo J. Y., Yeh K. W., Chen T. K., Huang T. W., Wu P. M., Lee Y. C., Huang Y. L., Chu Y. Y., Yan D. C. and Wu M. K., *Proc. Natl. Acad. Sci. U.S.A.*, **105** (2008) 14262.

[19] Shirage P. M., Kihou K., Lee C. H., Kito H., Eisaki H. and Iyo A., *J. Am. Chem. Soc.*, **133** (2011) 9630.

[20] Zhu X. Y., Han F., Mu G., Cheng P., Shen B., Zeng B. and Wen H. H., *Phys. Rev. B*, **79** (2009) 220512(R).

[21] Man H. Y., Qin C., Ding C., Wang Q., Gong X., Guo S. L., Wang H. D., Chen B. and Ning F. L., *EPL*, **105** (2014) 67004.

[22] Wang Q., Ning F. L. *et al.*, in preparation.

[23] Ding C., Qin C., Man H. Y., Imai T. and Ning F. L., *Phys. Rev. B*, **88** (2013) 041108(R).

[24] Kayanuma K., Kawamura R., Hiramatsu H. *et al.*, *Thin Solid Films*, **516** (2008) 5800.

[25] Emery N., Wildman E. J., Skakle J. M. S., Mclaughlin A. C., Smith R. I. and Fitch A. N., *Phys. Rev. B*, **83** (2011) 144429.